Combined Economic and Stability Analysis of a Microgrid: A Co-optimisation Approach

Carlos Sepulveda
Dep. Ingeniería Eléctrica
Universidad de Chile
Santiago, Chile

Rodrigo Moreno
Dep. Ingeniería Eléctrica
Universidad de Chile
& Imperial College London

Patricio Mendoza-Araya
Dep. Ingeniería Eléctrica
Universidad de Chile
Santiago, Chile

***Abstract*—Both economics and stability analysis are critical to operate electricity networks in an efficient and secure manner, especially in the context of microgrids, where more complex stability phenomena may arise. In this vein, we propose a combined economic and stability model implemented through a hierarchical approach, where a master problem determines the economic system dispatch regardless of stability considerations and then a slave subproblem attempts to stabilize the master's solution through the optimization of control gains. If the economic dispatch solution determined by the master problem cannot be stabilized by slave's adjustments of control gains, a feasibility cut is generated and added to the master problem to calculate a new, more stable dispatch solution (master and slave are run iteratively). We demonstrate that control gains can be co-optimized with power outputs of generating units (in real time) to obtain more economically efficient and secure dispatch solutions and therefore that economics and stability analysis can be combined in a single framework by using advanced optimization techniques.**

***Index Terms*—Energy management systems, Power system economics, Small signal stability, Co-optimization.**

I. Introduction

Microgrids have been recognized as a key component of the future smart grid, promoting the use of distributed energy resources, participating in an ancillary service market at the distribution level, and providing black start capability through the islanding operation ability [1, 2]. Even though microgrids could provide these features simultaneously, in the present operational paradigm, power system economics and stability are treated as different problems with their own technical frameworks and mathematical models. In this context, optimization, economic dispatch models are used to determine cost-effective system operation, while small signal models (among others) are used to determine stable operation. The economic dispatch problems usually take the form of an optimal power flow (OPF) problem with non-linear programming (NLP) formulation, where the nonlinearities come, for example, from the AC power flow equations. The small signal models are often obtained from a state-space representation of the microgrid, potentially using full-featured models that include detailed control laws such as the popular droop control [3].

Economic optimization and system stability may present conflicts, especially in the microgrid context, where stability can be significantly sensitive to the outputs of the economic dispatch. In fact, although system stability can be efficiently managed through control gains and control laws [4, 5, 6, 7], generation outputs can also affect the degree of stability of a given operating point. Therefore, there is an important opportunity to coordinate economic and stability decisions in a single mathematical framework.

Economic optimization with stability constraints has been studied earlier in both the main power system [8, 9, 10, 11] and the microgrid [12, 13, 14]. In the particular case of microgrids, previous works have focused on angle stability in unbalanced operation [13], uncertainty under intermittent generation [14], transient stability constrained OPF [11], among other aspects. However, scarce literature is found on small signal stability being co-optimized along with the economic dispatch. Reference [12] pursues the latter, but simplifies on the droop control gains that are chosen to be identical for all generators. In practice, there are several ways to choose the droop control gain, with the selection of gains proportional to power ratings being one of the most popular [3]. However, this selection of gains does not necessarily guarantee a stable operation at all times.

In this context, this paper presents a novel approach with a particular focus on small-signal stability and the use of feasibility cuts to iteratively eliminate regions of the OPF's searching space where solutions become unstable. Thus, the proposed economic dispatch model can simultaneously co-optimize generating units' outputs and gains in a real-time fashion (e.g., every 5 mins in an Energy Management System). The optimization is performed using a NLP formulation with added Benders cuts [15]. Particularly, our approach is divided into two stages or modules: (1) a master module that determines the optimal power flow (OPF) solution of the microgrid in a given operating conditions, and a (2) slave module that checks whether the obtained solution in (1) is stable (i.e., real parts of eigenvalues are negative). If the dispatch solution is unstable, control droops' gains are iteratively changed so as to minimize the maximum real part across all eigenvalues. If the dispatch solution remains unstable, the slave module generates a feasibility cut that is

C. Sepulveda, R. Moreno and P. Mendoza-Araya are with the University of Chile. R. Moreno is also with Imperial College London (corresponding author's email: rmorenovieyra@ing.uchile.cl).

incorporated in the master module to reduce its searching space (making the current solution unfeasible) and thus obtain a new, more stable solution in the next iteration. This process is illustrated in Fig.1.

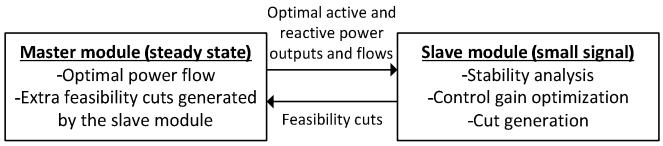

Fig: 1: Overview of proposed co-optimization approach.

Note that as the slave module may define a non-convex region, adding feasibility cuts to the master module (from the salve module) does not ensure global optimal to be found. The proposed approach, nevertheless, presents a workable option to coordinate complex decisions in economics and stability analysis that are usually decoupled, truly attempting to co-optimize generation power outputs and control gains. It is important to point out that, in practice, when an OPF solution is unstable, a new dispatch solution is determined by using *ad-hoc* engineering insights and heuristics methods. In this context, our proposed approach represents an improvement and this is demonstrated next through two case studies.

The organization of this paper is as follows. Section II introduces the proposed co-optimization problem, with the details on how the small-signal stability is introduced into the economic dispatch, OPF problem. Section III presents a hierarchical approach to solve this co-optimization problem. Section IV presents the optimization results over two case studies that exemplify the proposed co-optimization approach. Finally, conclusions are presented in Section V.

II. Co-optimization approach

The combined economic-stability problem can be formalized as shown in (1), where bold fonts refer to vectors.

$$\begin{aligned} &\min_{\boldsymbol{P},\boldsymbol{Q},\boldsymbol{V},\boldsymbol{\theta},\boldsymbol{k_P}} c(\boldsymbol{P}) \\ &s.t: \\ &\boldsymbol{P}-\boldsymbol{P_D}=\boldsymbol{I_P}(\boldsymbol{V},\boldsymbol{\theta}) \\ &\boldsymbol{Q}-\boldsymbol{Q_D}=\boldsymbol{I_Q}(\boldsymbol{V},\boldsymbol{\theta}) \\ &\boldsymbol{0}\le\boldsymbol{P}\le\overline{\boldsymbol{P}} \\ &\underline{\boldsymbol{Q}}\le\boldsymbol{Q}\le\overline{\boldsymbol{Q}} \\ &\underline{\boldsymbol{V}}\le\boldsymbol{V}\le\overline{\boldsymbol{V}} \\ &\underline{\boldsymbol{\theta}}\le\boldsymbol{\theta}\le\overline{\boldsymbol{\theta}} \\ &\underline{\boldsymbol{k_P}}\le\boldsymbol{k_P}\le\overline{\boldsymbol{k_P}} \\ &\hat{g}(\boldsymbol{P},\boldsymbol{Q},\boldsymbol{V},\boldsymbol{\theta},\boldsymbol{k_P},\boldsymbol{P_D},\boldsymbol{Q_D})\le 0 \end{aligned} \tag{1}$$

In (1), $c(\cdot)$ is the generation cost function. $\boldsymbol{I_P}(\cdot)$ and $\boldsymbol{I_Q}(\cdot)$ are the AC load flow equations, written as functions of voltages $\boldsymbol{V}$ and angles $\boldsymbol{\theta}$, where $\underline{\boldsymbol{V}},\overline{\boldsymbol{V}}$ and $\underline{\boldsymbol{\theta}},\overline{\boldsymbol{\theta}}$ represent their lower and upper bound limits, respectively. $\boldsymbol{P},\boldsymbol{Q}$ and $\overline{\boldsymbol{P}},\overline{\boldsymbol{Q}}$ are the generation outputs (active and reactive power) and the corresponding capacities (active and reactive power), respectively. $\underline{\boldsymbol{Q}}$ represents the lower bound limits for reactive powers. $\boldsymbol{k_P}$ contains the droop control gains of generating units, while $\overline{\boldsymbol{k_P}}$ and $\underline{\boldsymbol{k_P}}$ are the maximum and minimum values of droop control gains. Values in vectors $\boldsymbol{P_D}$ and $\boldsymbol{Q_D}$ refer to demand (active and reactive power). For the sake of simplicity, length of all vectors is equal to the number of busbars and we assume one generating unit (and demand) per busbar and no transmission capacity constraints. Note that this is to simplify the notation and does not represent a limitation of our approach. Additionally, $\hat{g}(\boldsymbol{P},\boldsymbol{Q},\boldsymbol{V},\boldsymbol{\theta},\boldsymbol{k_P},\boldsymbol{P_D},\boldsymbol{Q_D})\le 0$ (that is defined in (2)) represents the stability constraint, where scalar function $g(\cdot)$ corresponds to the maximum real part among all eigenvalues. α is a positive security margin to ensure that value of $g(\cdot)$ is not only negative but also far from zero.

$$\begin{aligned} &\hat{g}(\boldsymbol{P},\boldsymbol{Q},\boldsymbol{V},\boldsymbol{\theta},\boldsymbol{k_P},\boldsymbol{P_D},\boldsymbol{Q_D}) \\ &\qquad = \alpha + g(\boldsymbol{P},\boldsymbol{Q},\boldsymbol{V},\boldsymbol{\theta},\boldsymbol{k_P},\boldsymbol{P_D},\boldsymbol{Q_D}) \end{aligned} \tag{2}$$

III. Hierarchical approach

Our hierarchical approach (shown in (3) and (4)) is composed of a (i) master, economic module (shown in (3)) that determines the most economically efficient dispatch solution of a microgrid for a given operating condition (e.g., an hour), and (ii) a slave, stability module (shown in (4)) that determines optimal $\boldsymbol{k_P}$ for the given optimal values of $\boldsymbol{P}^*,\boldsymbol{Q}^*,\boldsymbol{V}^*,\boldsymbol{\theta}^*$ (determined by the master module; asterisk "*" refers to optimal values) to minimize $\hat{g}(\boldsymbol{P},\boldsymbol{Q},\boldsymbol{V},\boldsymbol{\theta},\boldsymbol{k_P},\boldsymbol{P_D},\boldsymbol{Q_D})$, which attempts to make the dispatch solution found by the master module stable from a small-signal stability perspective.

$$\begin{aligned} &\min_{\boldsymbol{P},\boldsymbol{Q},\boldsymbol{V},\boldsymbol{\theta}} c(\boldsymbol{P}) \\ &s.t: \\ &\boldsymbol{P}-\boldsymbol{P_D}=\boldsymbol{I_P}(\boldsymbol{V},\boldsymbol{\theta}) \\ &\boldsymbol{Q}-\boldsymbol{Q_D}=\boldsymbol{I_Q}(\boldsymbol{V},\boldsymbol{\theta}) \\ &\boldsymbol{0}\le\boldsymbol{P}\le\overline{\boldsymbol{P}} \\ &\underline{\boldsymbol{Q}}\le\boldsymbol{Q}\le\overline{\boldsymbol{Q}} \\ &\underline{\boldsymbol{V}}\le\boldsymbol{V}\le\overline{\boldsymbol{V}} \\ &\underline{\boldsymbol{\theta}}\le\boldsymbol{\theta}\le\overline{\boldsymbol{\theta}} \end{aligned} \tag{3}$$

$$\begin{aligned} &\min_{\boldsymbol{k_P}} \hat{g}(\boldsymbol{P}^*,\boldsymbol{Q}^*,\boldsymbol{V}^*,\boldsymbol{\theta}^*,\boldsymbol{k_P},\boldsymbol{P_D},\boldsymbol{Q_D}) \\ &\qquad s.t: \\ &\qquad \underline{\boldsymbol{k_P}}\le\boldsymbol{k_P}\le\overline{\boldsymbol{k_P}} \end{aligned} \tag{4}$$

Hence, the slave module stabilizes the dispatch solution determine by the master problem if $\hat{g}(\cdot)\le 0$. If the dispatch solution cannot be stabilized, an iterative process starts where a feasibility cut is generated and send to the master module in the form of a new linear constraint that will reduce the searching space of the OPF problem and make its new solution different to the previous one. The new solution is obtained while moving away from the previous one in the direction that makes $\hat{g}(\cdot)$ smaller. The feasibility cut can be written as shown in (5) and is obtained by solving the optimization problem shown in (4), where $\boldsymbol{\pi_P^T}$ is the (transposed) objective function's gradient vector associated with $\boldsymbol{P}^*,\boldsymbol{Q}^*,\boldsymbol{V}^*,\boldsymbol{\theta}^*$, when $\boldsymbol{k_P}^*$ is optimal. Note that (5) is the linear, first order Taylor approximation of $\hat{g}(\boldsymbol{P},\boldsymbol{Q},\boldsymbol{V},\boldsymbol{\theta},\boldsymbol{k_P},\boldsymbol{P_D},\boldsymbol{Q_D})\le 0$.

$$\hat{g}(\boldsymbol{P}^*, \boldsymbol{Q}^*, \boldsymbol{V}^*, \boldsymbol{\theta}^*, \boldsymbol{k_P}^*, \boldsymbol{P_D}, \boldsymbol{Q_D}) + \boldsymbol{\pi}_{\boldsymbol{P}}^T \begin{pmatrix} \boldsymbol{P} - \boldsymbol{P}^* \\ \boldsymbol{Q} - \boldsymbol{Q}^* \\ \boldsymbol{V} - \boldsymbol{V}^* \\ \boldsymbol{\theta} - \boldsymbol{\theta}^* \end{pmatrix} \leq 0 \quad (5)$$

Note that while the master problem (including its feasibility cuts) is solved through a NLP solver, the slave suproblem that represents the stabiliy part, is solved through an optimization-via-simulation approach.

IV. Co-Optimization Results

This section introduces two case studies. The first case presents a two-source microgrid that supplies a single load. The purpose of the first case is to illustrate the co-optimization approach within a simple system and hence we neglect the effect of network losses and reactive power. The second case presents a more realistic three-source microgrid with multiple loads and full consideration of losses and reactive power.

A. Two-source microgrid

In this microgrid, both sources are distributed generators (DG) connected to a common point (through power lines), at which the load is located. We consider an energy storage unit and a wind turbine as generation resources, as shown in Fig. 2(a). From the optimization point of view, we are interested in understanding how the low cost, but electrically far wind turbine is capable to provide maximum output (i.e., no wind curtailment) without compromising the stability of the system. Note that the marginal cost of the storage unit is not necessarily zero and, in fact, can be significantly higher [16].

The circuit diagram for this case study is shown in Fig. 2(b). As suggested by [17], we use dynamic phasor modeling for the generation units and load, which comprises two generation units coupled by R-L impedances (where R-L contains both coupling and line impedances), and includes droop control in both of them. The model for a single DG is simplified as an ideal voltage source with frequency droop control. The transfer function of this simple model is presented in (6), where the input is the point of coupling (PoC) voltage and the output is the current. Also, $\tilde{Y}$ is the small signal admittance, Z and φ are the coupling (and line) impedance magnitude and phase angle (consisting of equivalent R and L), V_e^A and V_L^A are the steady-state voltage amplitudes of the source and the PoC, with ϕ_e and ϕ_L their respective angles, and k_P is the droop control gain. Additionally, $\delta = \phi_L - \phi_e$ and U refers to the amplitude of phasor $\bar{V}_e - \bar{V}_L$ ($\bar{V}_e$ and $\bar{V}_L$ are shown in Fig. 2(b)).

This system's root loci is shown in Fig. 3, where we consider a demand of 1.2 [kW], a given dispatch condition (not the optimal), and a range of values for the control gain of source 1. The control gain of source 2 is not changed and kept equal to 1%. Note that Fig. 3 clearly shows that the system is stable for the control gains assessed at the selected dispatch condition, albeit roots' real parts can get very close to zero. Thus, we are interested in obtaining a new dispatch solution with an increased security margin of -32 ($\alpha = 32$, which means that the maximum real part across all eigenvalues cannot be higher than -32).

$$\begin{aligned}\tilde{Y}(s) = -\frac{1}{\Delta(s)} \cdot \frac{1}{Z} \Big[& \frac{Z}{L} \cos\phi_L \, s^2 \\ & + \frac{1}{L^2}\Big(Z^2 \cos(\phi_L - \varphi) \\ & - \frac{1}{2} L k_P V_e^A U \sin\phi_e \cos\phi_L\Big) s \\ & + \frac{1}{2L^2} Z k_P V_e^A (V_L^A \sin\phi_L \\ & + U \sin(\varphi - \phi_e) \cos\phi_L) \Big] \end{aligned} \quad (6)$$

$$\begin{aligned}\Delta(s) = s^3 + \frac{2R}{L} s^2 & \\ & + \frac{1}{L^2}\Big(Z^2 + \frac{1}{2} L k_P V_e^A V_L^A \sin(\delta)\Big) s \\ & + \frac{1}{2L^2} Z k_P V_e^A V_L^A \sin(\delta - \varphi)\end{aligned}$$

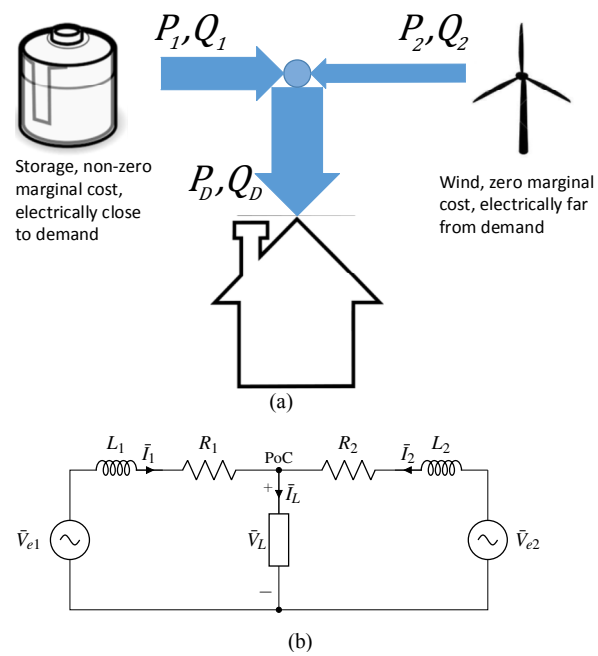

Fig. 2: Illustrative microgrid (a) and its electric schematic (b).

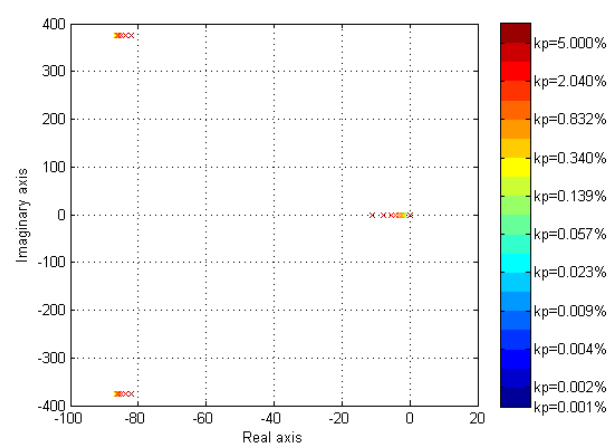

Fig. 3: Eigenvalues of the two-source system for various droop control gains of source 1 (region of interest plotted).

Hence, we apply our approach where the master module attempts to minimize costs, which, in this case, is equivalent to maximizing the output of the wind turbine (for the sake of simplicity, we assume that wind power generation is sufficient to supply demand). The results of the proposed iterative process are displayed in Table I, where due to its illustrative purpose, resistances and reactive powers have been neglected (i.e., linear or DC-OPF).

TABLE I. ITERATIONS RESULTS FOR THE CO-OPTIMIZATION APPROACH

Feasibility cuts	DG 1 [W]	DG 2 [W]	min $g(\cdot)$
0	0	1,200	-28.69
1	317	883	-31.04
2	499	701	-31.77
3	579	621	-31.96
4	599	601	-31.99
5	600	600	-32.00

The above results can be also observed in Fig. 4 that shows $g(\cdot)$ as a function of the energy storage's power output (note that to draw the black line, we evaluate $g(\cdot)$ several times in a process outside the proposed method). This figure illustrates that the most economically efficient solution proposed by the master module in the first iteration (storage output equal to 0 [W]) is infeasible (for any vector k_P), presenting eigenvalues (real part) that are higher than -32 (which is our arbitrary security margin). Thus, the stability of the microgrid has to be improved by increasing storage output and curtailing wind. This is introduced through a feasibility cut, shown in red color in Fig. 4. As the iteration continues, more feasibility cuts are introduced, until the optimal solution is found at iteration 5 (see number of blue dots on the black curve in Fig. 4). Interestingly, in this case $g(\cdot)$ corresponds to a convex function and therefore approximations through linear feasibility cuts can successfully find the true global optimal solution of the DC-OPF problem with stability constraints.

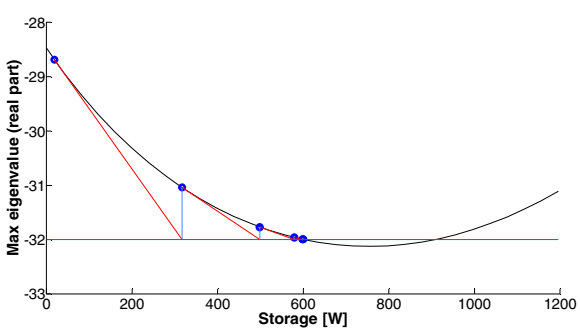

Fig. 4: Max eigenvalue (real part) as a function of the power output of the energy storage unit. Red lines represent the feasibility cuts in every iteration.

The progress of the Eigenvalues across the iterative process is shown in Fig. 5 in a root loci plot, demonstrating that the iterative process is effective in delivering more stable solutions.

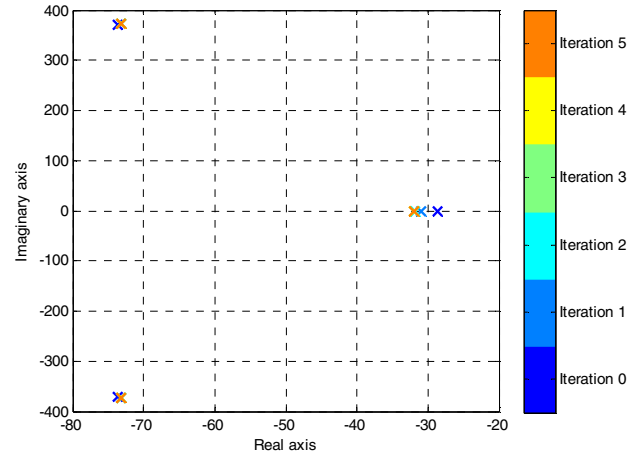

Fig. 5: Eigenvalues of the two-source system across the iterative process (region of interest plotted).

B. *Three-source microgrid*

This case study uses the same grid topology presented in [12], maintaining its line parameters but differing on the loads. This grid is shown in Fig. 5, where D_1 and D_3 represent constant impedance loads. The generators are modeled with droop gains between 0.01% and 5%.

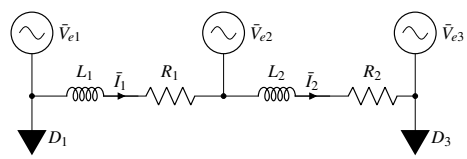

Fig. 5: Diagram of the three-source microgrid. Each generator is connected to the microgrid through the same coupling impedance R_C-L_C (see Table II).

The electrical parameters of this grid are presented in Table II. The variable costs for the DG units follow the expression

$$c(\boldsymbol{P}) = \boldsymbol{A}^{\boldsymbol{T}} \cdot \boldsymbol{P} + \boldsymbol{B}^{\boldsymbol{T}} \cdot \boldsymbol{P}^2 \tag{7}$$

where $c(\boldsymbol{P})$ is the resulting cost, $\boldsymbol{P}$ is the dispatched active power vector, $\boldsymbol{A}$ and $\boldsymbol{B}$ are the vectors with the cost function parameters shown in Table III, and function $(\cdot)^2$ outputs a vector where each element of the input vector are squared. Finally, upper and lower bounds are presented in Table IV.

In the first iteration, where the stability considerations are fully ignored, the OPF solution obtained does not meet the level of stability required (where $\alpha = 20$ is arbitrarily defined) and this is shown in the second column of Table V (labeled as *Initial solution*). However, when feasibility cuts are progressively included in the economic optimization, we can observe a significant improvement of the solution shown in the third column of Table V (labeled as *Final solution*). This table shows the comparison between both cases, how the resulting power flow differs, and how the total cost of the system changes. It takes seven feasibility cuts to reach the final power flow solution that meets the security margin of $\alpha = 20$. Table V also demonstrates how critical (for the purposes of stability) the reactive power dispatch is. There is a radical change on the reactive power dispatch of DGs 1, 2 and 3, and, to a lesser extent, on active power.

TABLE II. ELECTRICAL PARAMETERS FOR THE THREE-SOURCE MICROGRID

Variable	Symbol	Value
Base power	S_b	$100[VA]$
Rated voltage	V_b	$220[V]$
Rated frequency	f_0	$60[Hz]$
Resistance of line 1-2	R_1	$0.46[\Omega]$
Reactance of line 1-2	X_1	$0.20[\Omega]$
Resistance of line 2-3	R_2	$0.70[\Omega]$
Reactance of line 2-3	X_2	$1.16[\Omega]$
Coupling resistance	R_c	$0.03[\Omega]$
Coupling reactance	L_c	$0.35[mH]$
Demand at busbar 1	D_1	$500[W]$
Demand at busbar 3	D_3	$8{,}500[W]$

TABLE III. COST FUNCTION PARAMETERS FOR THE MICROGRID DGS

DG	Quadratic part (B)	Linear part (A)
1	0.135	50
2	0.310	70
3	1.831	100

TABLE IV. CONSTRAINTS FOR THE DGS VARIABLES

Variable	Minimum value	Maximum value
P_1	$0[W]$	$8{,}000[W]$
P_2	$0[W]$	$8{,}500[W]$
P_3	$0[W]$	$7{,}500[W]$
V_1, V_2, V_3	$0.9[pu]$	$1.1[pu]$
$\theta_1, \theta_2, \theta_3$	$-70º$	$70º$
$k_{P_1}, k_{P_2}, k_{P_3}$	0.01%	5%

TABLE V. COMPARISON OF THE OPTIMIZATION WITHOUT AND WITH SMALL-SIGNAL STABILITY CONSTRAINTS

Variable	Initial solution (w/o stability constraints)	Final solution (w/ stability constraints)	Change [%]
α	20.00		
$P_1[W]$	5,306	5,034	-5
$P_2[W]$	2,508	2,568	$+2$
$P_3[W]$	519	743	$+43$
$Q_1[VAr]$	-133	1,444	$-1{,}186$
$Q_2[VAr]$	1,044	$-2{,}366$	-327
$Q_3[VAr]$	380	2,288	$+502$
$V_1[pu]$	1.05	1.00	-5
$V_2[pu]$	1.00	0.96	-4
$V_3[pu]$	0.90	0.90	0
$\theta_1[º]$	1.14	0.30	-74
$\theta_2[º]$	0.00	0.00	0
$\theta_3[º]$	-10	-12	$+20$
$min\ g(\cdot)$	-9.60	-20	$+108$
Cost [$]	6,735,615	6,981,681	$+4$

V. CONCLUSIONS

The proposed economic-stability approach to solve an economic dispatch with stability constraints has been successfully applied on two case studies, which demonstrate that economic and stability analysis can be combined by using advanced optimization techniques. We illustrate the performance of our approach, demonstrating that an economic and stable solution can be reached through a unified mathematical program, eliminating the need to apply separate engineering insights/arbitrary rules to stabilize system operation outside the economic dispatch problem.

VI. REFERENCES

[1] C. Yuen and A. Oudalov, "The Feasibility and Profitability of Ancillary Services Provision from Multi-MicroGrids," in *2007 IEEE Lausanne Power Tech*, Lausanne, 2007.

[2] M. Amin, "The Power of Microgrids," *Electricity Today T&D Magazine,* pp. 48-53, Jan/Feb/Mar 2016.

[3] D. Olivares, A. Mehrizi-Sani, A. Etemadi, C. Canizares, R. Iravani, M. Kazerani, A. Hajimiragha, O. Gomis-Bellmunt, M. Saeedifard, R. Palma-Behnke, G. Jimenez-Estevez and N. Hatziargyriou, "Trends in Microgrid Control," *IEEE Transactions on Smart Grid,* vol. 5, no. 4, pp. 1905-1919, July 2014.

[4] N. Pogaku, M. Prodanovic and T. Green, "Modeling, Analisys and Testing of Autonomous Operation of an Inverter-Based Microgrid," *IEEE Transactions on Power Electronics,* vol. 22, no. 2, pp. 613 - 625, 2007.

[5] X. Wang, F. Zhuo, H. Guo, L. Meng, L. Yang and J. Liu, "Stability analisys of droop control for inverter using dynamic phasors method," in *Energy Conversion Congress and Exposition (ECCE)*, Phoenix, AZ, 2011.

[6] R. Majumder, B. Chaudhuri, A. Ghosh, R. Majumder, G. Ledwich and F. Zare, "Improvement of Stability and Load Sharing in an Autonomous Microgrid Using Supplementary Droop Control Loop," *IEEE Transactions on Power Systems,* vol. 25, no. 2, pp. 796 - 808, 2009.

[7] M. Erickson, T. Jahns and R. Lasseter, "Improved power control bandwidth of grid-forming sources in a CERTS microgrid," in *Energy Conversion Congress and Exposition (ECCE), 2012 IEEE*, Raleigh, NC, 2012.

[8] Y. Pipelzadeh, R. Moreno, B. Chaudhuri, G. Strbac and T. C. Green, "Corrective Control With Transient Assistive Measures: Value Assessment for Great Britain Transmission System," *IEEE Transactions on Power Systems,* vol. 32, no. 2, pp. 1638-1650, March 2017.

[9] R. Avalos, C. Cañizares and M. Anjos, "A practical voltage-stability-constrained optimal power flow," in *Power and Energy Society General Meeting - Conversion and Delivery of Electrical Energy in the 21st Century, 2008 IEEE*, Pittsburgh, PA, 2008.

[10] A. Pizarro-Martinez, C. Fuerte-Esquivel and D. Ruiz-Vega, "A New Practical Approach to Transient Stability-Constrained Optimal Power Flow," *IEEE Transactions on Power Systems,* vol. 26, no. 3, pp. 1686 - 1696, 2011.

[11] R. Zarate-Minano, T. Van Cutsem, F. Milano and A. Conejo, "Securing Transient Stability Using Time-Domain Simulations Within an Optimal Power Flow," *IEEE Transactions on Power Systems,* vol. 25, no. 1, pp. 243 - 253, 2009.

[12] E. Barklund, N. Pogaku, M. Prodanovic, C. Hernandez-Aramburo and T. Green, "Energy Management in Autonomous Microgrid Using Stability-Constrained Droop Control of Inverters," *IEEE Transactions On Power Electronics,* vol. 23, no. 5, pp. 2346 - 2352, 2008.

[13] E. Dall'Anese, Z. Hao and G. Giannakis, "Distributed Optimal Power Flow for Smart Microgrids," *IEEE Transactions on Smart Grid,* vol. 4, no. 3, pp. 1464 - 1475, 2013.

[14] D. Olivares, J. D. Lara, C. Canizares and M. Kazerani, "Stochastic-Predictive Energy Management System for Isolated Microgrids," *IEEE Transactions on Smart Grid,* vol. 6, no. 6, pp. 2681 - 2693, 2015.

[15] A. Geoffrion, "Generalized benders decomposition," *Journal of optimization theory and applications,* vol. 10, no. 4, pp. 237-260, Oct 1972.

[16] M. Pereira and L. Pinto, "Multi-stage stochastic optimization applied to energy planning," vol. 52, no. 1-3, pp. 359-375, 1991.

[17] P. A. Mendoza-Araya and G. Venkataramanan, "Stability Analysis of AC Microgrids Using Incremental Phasor Impedance Matching," *Electric Power Components And Systems,* vol. 43, no. 4, pp. 473-484, Feb 2015.